Editors' Suggestion

Observation of Collisions between Two Ultracold Ground-State CaF Molecules

Lawrence W. Cheuk,[1,2,3,*] Loïc Anderegg,[1,2] Yicheng Bao,[1,2] Sean Burchesky,[1,2] Scarlett S. Yu,[1,2] Wolfgang Ketterle,[2,4] Kang-Kuen Ni,[1,2,5] and John M. Doyle[1,2]

[1]*Department of Physics, Harvard University, Cambridge, Massachusetts 02138, USA*
[2]*Harvard-MIT Center for Ultracold Atoms, Cambridge, Massachusetts 02138, USA*
[3]*Department of Physics, Princeton University, Princeton, New Jersey 08544, USA*
[4]*Department of Physics, Massachusetts Institute of Technology, Cambridge, Massachusetts 02139, USA*
[5]*Department of Chemistry and Chemical Biology, Harvard University, Cambridge, Massachusetts 02138, USA*

(Received 4 February 2020; revised 7 May 2020; accepted 29 June 2020; published 20 July 2020; corrected 3 March 2021)

We measure inelastic collisions between ultracold CaF molecules by combining two optical tweezers, each containing a single molecule. We observe collisions between $^2\Sigma$ CaF molecules in the absolute ground state $|X, v = 0, N = 0, F = 0\rangle$, and in excited hyperfine and rotational states. In the absolute ground state, we find a two-body loss rate of $1.4(8) \times 10^{-10}$ cm^3/s, which is below, but close to, the predicted universal loss rate.

DOI: 10.1103/PhysRevLett.125.043401

The rich internal structure of molecules has led to many proposed applications ranging from precision measurements that probe beyond standard model physics to quantum simulation of condensed matter models and quantum computation [1]. In the past decade, experimental advances in the production and control of molecules have brought many of the proposed applications within reach. These advances include coherent assembly of diatomic molecules from ultracold atoms [2–7], laser cooling of molecules to μK temperatures [8–11], and coherent control of internal molecular states [12–20].

Beyond controlling the internal states and the motion of molecules, an important research frontier is to understand and control how they interact. Along this front, how molecules collide is of central importance. Favorable collisional properties, i.e., high elastic scattering rate compared to inelastic loss rate [21,22], could lead to direct evaporative cooling of molecular gases to quantum degeneracy. Full understanding of molecular collisions could also allow one to tune the elastic [23–25] and inelastic scattering rates [26–29] by applying external fields. Furthermore, by elucidating the role of specific quantum states and quantum statistics of the reactants [1,30,31], collisions in the ultracold regime provide important insights into chemical and inelastic processes. For example, recent experiments have provided evidence for sticky collisions and long-lived complexes for both reactive and nonreactive molecules [32–34].

Experimentally, inelastic collisional (loss) rates have been measured in many bi-alkali molecules either in the $^1\Sigma$ ground state or the metastable $^3\Sigma$ state, including ^{40}K^{87}Rb [2], ^{23}Na^{40}K [5], ^{6}Li^{23}Na [7], ^{23}Na^{87}Rb [32], ^{87}Rb^{133}Cs [4,13,33], and ^{87}Rb$_2$ [35]. For chemically reactive species, two molecules are likely lost when they reach distances much shorter than the van der Waals length $l_{\mathrm{vdW}} = (mC_6/\hbar^2)^{1/4}$, where C_6 is the van der Waals coefficient and m is the molecular mass. Experiments with chemically reactive species have observed loss rates similar to those estimated by universal loss models, where the short-range loss probability is unity. Surprisingly, even for chemically nonreactive molecules, experiments have also reported loss rates within a factor of unity of universal loss, which has been interpreted as evidence for "sticky collisions," where a dense spectrum of molecular resonances leads to enhanced losses that approach the universal rate [36,37]. These observations illustrate that even collisions between simple, nonreactive diatomic molecules can exhibit qualitatively new features not found in atomic collisions.

Recently, direct laser cooling and trapping of molecules [8–11,17,38–42] have opened the door to studying $^2\Sigma$ molecules in the ultracold regime. Compared to ground state bialkali molecules, the unpaired electron spin in diatomic $X^2\Sigma$ molecules leads to a much larger hyperfine structure and additional features such as electron-spin-rotational coupling and intermolecular electronic spin-spin interactions at long ranges. In a previous study of bulk samples of rotationally excited $^2\Sigma$ CaF molecules, collisional loss rates near the Langevin limit were observed [42]. However, the method used could neither fully control the internal state nor the exact number of molecules. One could therefore not easily distinguish between various loss mechanisms such as hyperfine and rotational relaxation.

In this Letter, we have developed an optical tweezer-based approach for studying collisions in laser-cooled CaF molecules, which are chemically reactive. This provides full control of the number of molecules and their internal state, overcoming previous limitations. Specifically, we

prepare two single molecules in separate optical tweezer traps, initialize them in the same internal state, and then merge them into a single trap, thereby creating an exact two-body collisional system. Our approach ensures, by construction, that only single-body and two-body processes are at play, in contrast to previous measurements in bulk molecular gases. We note that with atoms, similar tweezer-based approaches have been used to probe hyperfine relaxation [43,44], coherent two-body dynamics [45], and Feshbach resonances [46].

The starting point of our experiment is a magneto-optical trap (MOT) of $^{40}Ca^{19}F$ molecules, which are in a mixture of hyperfine states in the first excited rotational manifold ($|X, N = 1\rangle$). These molecules are then loaded with Λ cooling into an optical dipole trap (ODT) formed by a single focused beam of 1064 nm light [41]. Subsequently, single molecules are stochastically loaded into two optical tweezer traps in the presence of laser cooling light [42]. Both tweezers have a spot size of ~ 2 μm and trap depths of 1400 μK (see the Supplemental Material [47]). The position of the right tweezer trap is fixed, while the position of the left tweezer trap can be varied. The two tweezer traps are derived from a common laser source at 780 nm, which is split into two paths and recombined. One path passes through an acousto-optical deflector (AOD), where the radio frequency driving the AOD controls the position of the tweezer trap. The other path generates a stationary tweezer trap. The ~ 100 MHz frequency difference between the beams and their orthogonal linear polarizations eliminate parametric heating that could otherwise arise due to interference.

To study collisions, we overlap the two tweezer traps, which are each filled with at most one molecule. Since the loading is stochastic, i.e., each trap can be empty or filled, four possible initial configurations can be realized. To identify the initial configuration, we measure the individual trap occupations using a 30 ms pulse of Λ-imaging light. After detection, the molecules are brought into the desired internal state in the ground rotational manifold ($N = 0$) using optical and microwave pulses. The two tweezer traps are then overlapped by sweeping the left tweezer trap onto the stationary tweezer (right) over 1 ms. The movable trap is subsequently ramped down in 1 ms, slow enough to ensure adiabaticity. Following this merging step, both molecules are held together for a variable time in the stationary tweezer trap, during which collisions can occur. The merging process is then reversed, and the surviving molecules are transferred back into the $|N = 1\rangle$ state for subsequent detection. This splitting step is necessary. During imaging, two molecules within a single trap are rapidly lost due to light-induced collisions before they can be detected. Following splitting, a second image is taken to determine the final tweezer occupations. The intensities of the two tweezer traps are tuned such that during splitting, a molecule has equal probability of ending up in either trap.

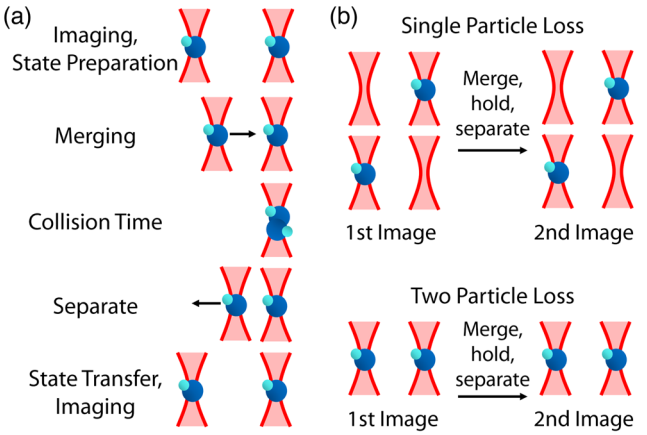

FIG. 1. Measuring collisional loss with two molecules. (a) Measurement protocol. The molecules are initially in $|N = 1\rangle$. A nondestructive image is taken to determine the tweezer occupations prior to state preparation and merging. The tweezers are merged for a variable hold time, and subsequently separated. The remaining molecules are transferred back to $|N = 1\rangle$ and a second image is taken. The total time between the two images is held constant. (b) Determining one-particle versus two-particle loss. To measure single-particle loss, we postselect for data where one molecule is detected in the first image and measure its survival probability in the second image. Similarly, for two-particle loss, we postselect for two molecules in the first image and measure the survival probability of both molecules in the second image.

If both molecules survive, they have a 50% chance of being in separate traps. By postselecting on the molecule number in the first image, we can extract the single-particle and two-particle loss rates. In detail, single-particle loss is observed by looking at data where one molecule is detected in the first image, and measuring its survival probability. Two-particle loss is observed by looking at data where two molecules are detected initially, and measuring the probability of both molecules surviving. By observing the single-particle and two-particle survival probabilities versus the time that the traps are merged, one obtains the corresponding loss rates. This measurement protocol for probing collisional loss is summarized in Fig. 1. In order to cancel effects due to single-particle loss (such as collisions with background gas), we keep the total time between the initial and final measurements constant, while varying the time that the traps are merged. The extracted single particle loss rate should therefore be consistent with zero. A nonzero two-particle loss rate would indicate that two-body collisional loss has occurred.

An important feature of our tweezer-based approach is the control over the internal molecular state. With single molecules in separate optical tweezers, light-assisted collisions, which typically lead to rapid losses at densities required to probe collisions, are absent. Optical preparation of the internal state thus becomes possible. We use a combination of optical pumping and microwave pulses to

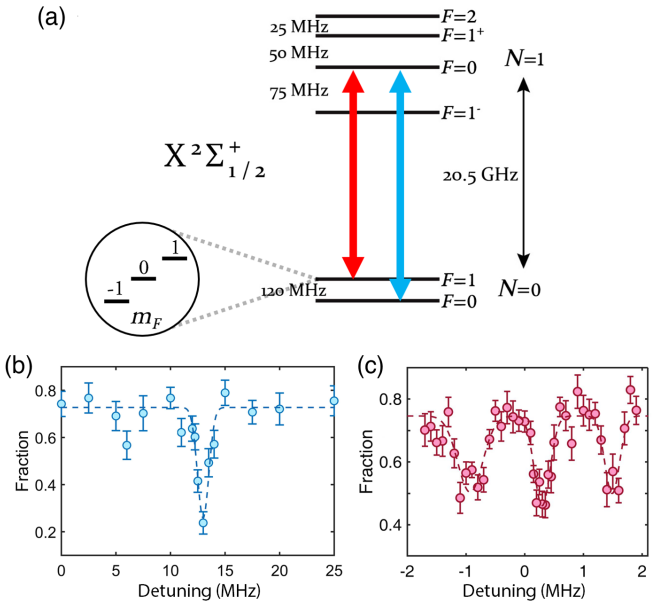

FIG. 2. Preparing molecules in the ground rotational manifold. (a) Rotational and hyperfine structure in the ground electronic and vibrational state of CaF ($X^2\Sigma, v = 0$). Molecules are initially prepared in $|N = 1, F = 0\rangle$ via optical pumping with 80% fidelity. Microwave pulses (red and blue arrows) can be applied to transfer molecules to the $|N = 0, F = 0\rangle$ or $|N = 0, F = 1\rangle$ manifolds. (b) Microwave spectroscopy of the absolute ground state $|N = 0, F = 0\rangle$. A Landau-Zener sweep is used to transfer molecules into $|N = 0, F = 0\rangle$. The applied microwave frequency is fixed, while the magnetic field is swept linearly over 2.5 G about the resonance (center at 3.5 G) in 20 ms. Shown is the remaining fraction of molecules in $|N = 1\rangle$ versus the applied microwave frequency for a fixed magnetic field sweep. (c) Microwave spectroscopy of the $|N = 0, F = 1\rangle$ manifold in a magnetic field of 1 G. A single microwave pulse is applied for 20 ms. Shown is the surviving fraction in the $|N = 1\rangle$ manifold. The three Zeeman levels ($m_F = -1, 0, 1$) are well resolved.

transfer the single molecules into the desired internal state before merging. In the following, we describe in detail how we bring the molecules into the rotational ground state, which consists of two hyperfine manifolds, $|N = 0, F = 0\rangle$ and $|N = 0, F = 1\rangle$ [Fig. 2(a)]. We optically pump into the $|N = 1, F = 0, m_F = 0\rangle$ state by applying 100 μs of light resonant with the $|X, v = 0, N = 1, F = 2, 1+, 1-\rangle \rightarrow |A, v = 0, N = 0, J = 1/2\rangle$ transitions. Subsequently, a microwave sweep or π pulse is applied to bring $|N = 1, F = 0, m_F = 0\rangle$ molecules into the desired hyperfine state in the $|N = 0\rangle$ rotational manifold. Although nominally forbidden, the $|N = 1, F = 0, m_F = 0\rangle \rightarrow |N = 0, F = 0, m_F = 0\rangle$ transition can be directly driven with microwaves when a weak magnetic field ($\sim$3 G) is applied. The magnetic field admixes the $|N = 0, F = 1, m_F = 0\rangle$ state [Fig. 2(b)], making the transition allowed. Due to the low resulting Rabi frequency $\sim 2\pi \times 2$ kHz, we used a Landau-Zener sweep implemented via a magnetic field sweep for robustness. The three Zeeman states of $|N = 0, F = 1\rangle$ can be resolved by applying a bias magnetic field [Fig. 2(c)]. For these states, where large Rabi frequencies $\sim 2\pi \times 100$ kHz are available, we use a single π pulse for transfer. We achieve transfer efficiencies of 74% into the absolute ground state ($|N = 0, F = 0, m_F = 0\rangle$), and 70% into the excited hyperfine manifold ($|N = 0, F = 1\rangle$) (see the Supplemental Material [47]). After optical pumping, any molecules remaining in $|N = 1\rangle$ are removed by a pulse of light resonant on the $|N = 1\rangle$ cycling transition, which heats $|N = 1\rangle$ molecules out of the trap. Since state preparation occurs after the initial image but before the traps are merged, imperfect transfer leads only to an overall reduction in the surviving fraction, and does not produce additional background.

For molecules in the absolute ground state $|N = 0, F = 0\rangle$, we measure a two-particle $1/e$ lifetime of 16 (3) ms, while single particle loss is indeed consistent with zero as expected from the measurement protocol [Figs. 3(a) and 3(b)]. The observed two particle loss is direct evidence of two-body collisions. Since rotational relaxation and hyperfine decay cannot occur in the absolute ground state, the loss is either due to the energetically allowed chemical reaction of $CaF + CaF \rightarrow CaF_2 + Ca$ [51,52], or formation of complexes that are either not detectable or quickly lost due to photoexcitation [53]. To extract a two-body loss rate constant, we determine the mean density of the tweezer trap by a Monte Carlo simulation using measured trap parameters and the molecular temperature [41(12) μK] measured via time-of-flight expansion (see the Supplemental Material [47]). The two-body loss rate constant for CaF molecules in the absolute ground state is found to be $1.4(8) \times 10^{-10}$ cm^3/s. We note that the temperature achieved is lower than the d-wave threshold (p-wave

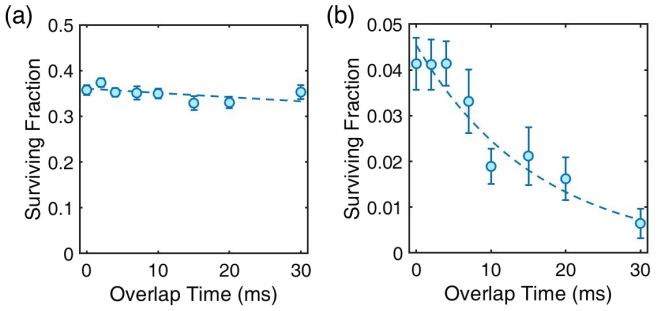

FIG. 3. Two-particle loss versus single-particle loss. In order to cancel out single-particle loss, the total time between the initial and final measurement is held constant, while the time that the traps are merged is varied. (a) One-particle loss measured by postselecting on data where a single molecule is loaded. An exponential fit to $Ae^{-\Gamma t}$ yields a loss rate Γ of 2.7(1.8) s^{-1} ($1/e$ lifetime $\sim$400 ms). This is consistent with no loss, which verifies that the measurement protocol cancels out single-particle loss. (b) Two-particle loss measured by post-selecting on data where two molecules are loaded. An exponential fit gives a time constant of 16(3)ms.

and d-wave thresholds at 20 and 106 μK, respectively). When prepared in identical internal states, p-wave scattering is absent due to the bosonic exchange statistics.

We next compare the loss rates to a single channel model [48,49] with universal loss, where molecules are lost with unit probability once they approach distances much smaller than the van der Waals length, $l_{\mathrm{vdW}} = (mC_6/\hbar^2)^{1/4}$. In the ground rotational manifold, the C_6 coefficient is identical for all internal states, and ignoring the small electronic contribution, is given by $C_6 = [1/(4\pi\epsilon_0)^2] \cdot d^4/(6B)$, where d is the dipole moment of the molecule and B the rotational constant. For CaF, both the dipole moment and rotational constant are large, with values of $d = 3.1$Debye and $B \approx 2\pi\hbar \times 10.15$ GHz, yielding a van der Waals length of $l_{\mathrm{vdW}} = 400a_0$, where a_0 is the Bohr radius. The corresponding universal loss rate is computed in a single-channel model [48] assuming unity loss at a short range. We sum over all partial waves [49] and average over a thermal distribution of collision energies [33] at the experimentally determined temperature of $41(12)$ μK. This yields a loss rate of $3.0(2) \times 10^{-10}$ cm^3/s, which is larger than but close to the measured value. Our results are similar to the case in bialkali molecules, where loss rates of the same order of magnitude as universal loss were observed [2,4,5,7,13,32,33,35].

As a next step, we have investigated whether the collisional loss rate depends on the spin state. Theoretical work on the $X^2\Sigma$ molecule SrF has indicated that in the energetically allowed chemical reaction of $\mathrm{SrF} + \mathrm{SrF} \rightarrow \mathrm{SrF_2} + \mathrm{Sr}$, only the singlet states of the trimer $\mathrm{SrF_2}$ can form [51]. Calculations of collisions between Li and the $X^2\Sigma$ molecules CaH [54] and SrOH [55] have also found that chemical reactions in the triplet channel are energetically forbidden at low temperatures, while reactions in the singlet channel proceed barrierlessly. In addition, the calculations predict slow spin relaxation rates, implying that when the atoms and molecules are both spin polarized in the triplet channel, inelastic loss due to chemical processes is strongly suppressed. These results suggest that spin-polarized CaF molecules could potentially have reduced inelastic losses compared to the unpolarized case, if the spin relaxation rate is similarly small. Although theoretical predictions CaF-CaF collisions are not available, we experimentally measured the two-body loss rate of spin-polarized CaF by preparing molecules in one of the stretched states at a finite magnetic field. The lower energy stretched state $|N = 0, F = 1, m_F = -1\rangle$ is used to suppress possible Zeeman relaxation within the same hyperfine manifold. At a magnetic field of 4 G, we find, within the experimental uncertainty, a loss rate constant identical to molecules in the absolute ground state $|N = 0, F = 0, m_F = 0\rangle$. We also measure a similar loss rate at a higher magnetic field of 8 G. We therefore conclude that collisional loss is not suppressed for spin-polarized molecules for the magnetic fields explored.

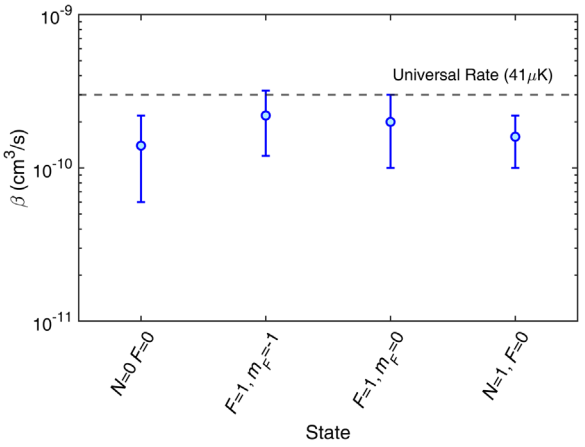

FIG. 4. Summary of collisional loss rates. Shown are the measured collisional loss rates of various hyperfine states in the ground and first excited rotational manifold. The universal loss rate at 40 μK is shown in dashed. For the states $|N = 0, F = 1, m_F = -1, 0\rangle$, the rates are measured at 8 G. The corresponding measured lifetimes are 16.3(4.0) ms, 10.8 (1.6) ms, 12.0(2.3) ms, and 14.8(4.0) ms for $|N = 0, F = 0\rangle$, $N = 0, F = 1, m_F = -1\rangle$, $|N = 0, F = 1, m_F = 0\rangle$, $|N = 0, F = 1, m_F = -1\rangle$, and $|N = 1, F = 0\rangle$, respectively. In addition, at the lower field of 4 G, the measured lifetime for $|N = 0, F = 1, m_F = -1\rangle$ is 10.6(2.0) ms. No significant dependence on spin polarization and hyperfine state is observed.

Compared to the absolute ground state, the spin-polarized molecules can be lost due to hyperfine relaxation. We next measured the hyperfine relaxation rate by preparing molecules in the non-spin-polarized state $|N = 0, F = 1, m_F = 0\rangle$. This yielded a similar value, indicating that either complex formation or chemical reactions occur much faster than hyperfine relaxation. Taken together, these results (summarized in Fig. 4) indicate that either the chemical reaction rate or complex formation rate is independent of spin in the range of magnetic fields explored.

In conclusion, we have developed an optical tweezer-based approach to study molecular collisions, which has allowed us to measure the collisional loss rates of $^2\Sigma$ CaF molecules in their absolute rovibrational ground state, as well as selected excited hyperfine states. The measurements indicate that the dominant loss mechanism is either chemical reactions or formation of complexes that are either not detected or quickly loss due to photoexcitation by the light used for optical trapping. These photo-induced losses [56] have in fact been observed in both RbCs and KRb recently [53,57], and could explain the losses observed here for CaF. In the regime of magnetic fields explored, the observed loss rates do not exhibit dependence on the hyperfine state, suggesting that the chemical reaction rate or the complex formation rate does not depend on the electronic spin of the molecules. In the future, collisional losses could be suppressed by implementing collisional

shielding schemes that prevent molecules from reaching short range [26–29]. Efficient suppression of collisional loss could open up new avenues of preparing quantum gases of molecules such as evaporative cooling [21,22] or algorithmic cooling that relies on interaction blockade [58]. The tweezer-based approach developed in this work will be well suited to exploring these possibilities. Our work can also be extended to more complex laser-coolable molecules including polyatomic ones [59], which could be a rich arena for explorations in ultracold collisions and reactions [1,30], as well as quantum simulation [60].

This work was supported by the NSF and ARO. We thank John Bohn, Tijs Karman and Goulven Quemener for insightful discussions and universal loss calculations. L. W. C. acknowledges support from the MPHQ. L. A. acknowledges support from HQI. S. B. and S. S. Y. acknowledge support from the NSF GRFP.

*lcheuk@princeton.edu

[1] L. D. Carr, D. DeMille, R. V. Krems, and J. Ye, New J. Phys. **11** (2009).
[2] K.-K. Ni, S. Ospelkaus, M. H. G. de Miranda, A. Pe'er, B. Neyenhuis, J. J. Zirbel, S. Kotochigova, P. S. Julienne, D. S. Jin, and J. Ye, Science **322**, 231 (2008).
[3] P. K. Molony, P. D. Gregory, Z. Ji, B. Lu, M. P. Köppinger, C. R. Le Sueur, C. L. Blackley, J. M. Hutson, and S. L. Cornish, Phys. Rev. Lett. **113**, 255301 (2014).
[4] T. Takekoshi, L. Reichsöllner, A. Schindewolf, J. M. Hutson, C. R. Le Sueur, O. Dulieu, F. Ferlaino, R. Grimm, and H.-C. Nägerl, Phys. Rev. Lett. **113**, 205301 (2014).
[5] J. W. Park, S. A. Will, and M. W. Zwierlein, Phys. Rev. Lett. **114**, 205302 (2015).
[6] M. Guo, R. Vexiau, B. Zhu, B. Lu, N. Bouloufa-Maafa, O. Dulieu, and D. Wang, Phys. Rev. A **96**, 052505 (2017).
[7] T. M. Rvachov, H. Son, A. T. Sommer, S. Ebadi, J. J. Park, M. W. Zwierlein, W. Ketterle, and A. O. Jamison, Phys. Rev. Lett. **119**, 143001 (2017).
[8] J. F. Barry, D. J. McCarron, E. B. Norrgard, M. H. Steinecker, and D. DeMille, Nature (London) **512**, 286 (2014).
[9] S. Truppe, H. J. Williams, M. Hambach, L. Caldwell, N. J. Fitch, E. A. Hinds, B. E. Sauer, and M. R. Tarbutt, Nat. Phys. **13**, 1173 (2017).
[10] L. Anderegg, B. L. Augenbraun, E. Chae, B. Hemmerling, N. R. Hutzler, A. Ravi, A. Collopy, J. Ye, W. Ketterle, and J. M. Doyle, Phys. Rev. Lett. **119**, 103201 (2017).
[11] A. L. Collopy, S. Ding, Y. Wu, I. A. Finneran, L. Anderegg, B. L. Augenbraun, J. M. Doyle, and J. Ye, Phys. Rev. Lett. **121**, 213201 (2018).
[12] S. Ospelkaus, K.-K. Ni, G. Quéméner, B. Neyenhuis, D. Wang, M. H. G. de Miranda, J. L. Bohn, J. Ye, and D. S. Jin, Phys. Rev. Lett. **104**, 030402 (2010).
[13] P. D. Gregory, J. Aldegunde, J. M. Hutson, and S. L. Cornish, Phys. Rev. A **94**, 041403(R) (2016).
[14] F. Wolf, Y. Wan, J. C. Heip, F. Gebert, C. Shi, and P. O. Schmidt, Nature (London) **530**, 457 (2016).
[15] J. W. Park, Z. Z. Yan, H. Loh, S. A. Will, and M. W. Zwierlein, Science **357**, 372 (2017).
[16] C.-w. Chou, C. Kurz, D. B. Hume, P. N. Plessow, D. R. Leibrandt, and D. Leibfried, Nature (London) **545**, 203 (2017).
[17] H. J. Williams, L. Caldwell, N. J. Fitch, S. Truppe, J. Rodewald, E. A. Hinds, B. E. Sauer, and M. R. Tarbutt, Phys. Rev. Lett. **120**, 163201 (2018).
[18] Y. Lin, D. R. Leibrandt, D. Leibfried, and C. wen Chou, Nature (London) **581**, 273 (2020).
[19] F. Seeßelberg, X.-Y. Luo, M. Li, R. Bause, S. Kotochigova, I. Bloch, and C. Gohle, Phys. Rev. Lett. **121**, 253401 (2018).
[20] M. Sinhal, Z. Meir, K. Najafian, G. Hegi, and S. Willitsch, Science **367**, 1213 (2020).
[21] B. K. Stuhl, M. T. Hummon, M. Yeo, G. Quéméner, J. L. Bohn, and J. Ye, Nature (London) **492**, 396 (2012).
[22] H. Son, J. J. Park, W. Ketterle, and A. O. Jamison, Nature (London) **580**, 197 (2020).
[23] J. L. Bohn, A. V. Avdeenkov, and M. P. Deskevich, Phys. Rev. Lett. **89**, 203202 (2002).
[24] L. Lassablière and G. Quéméner, Phys. Rev. Lett. **121**, 163402 (2018).
[25] A. Dawid, M. Lewenstein, and M. Tomza, Phys. Rev. A **97**, 063618 (2018).
[26] A. V. Gorshkov, P. Rabl, G. Pupillo, A. Micheli, P. Zoller, M. D. Lukin, and H. P. Büchler, Phys. Rev. Lett. **101**, 073201 (2008).
[27] G. Quéméner and J. L. Bohn, Phys. Rev. A **93**, 012704 (2016).
[28] M. L. González-Martínez, J. L. Bohn, and G. Quéméner, Phys. Rev. A **96**, 032718 (2017).
[29] T. Karman and J. M. Hutson, Phys. Rev. Lett. **121**, 163401 (2018).
[30] R. V. Krems, Phys. Chem. Chem. Phys. **10**, 4079 (2008).
[31] M. H. G. de Miranda, A. Chotia, B. Neyenhuis, D. Wang, G. Quéméner, S. Ospelkaus, J. L. Bohn, J. Ye, and D. S. Jin, Nat. Phys. **7**, 502 (2011).
[32] X. Ye, M. Guo, M. L. González-Martínez, G. Quéméner, and D. Wang, Sci. Adv. **4**, eaaq0083 (2018).
[33] P. D. Gregory, M. D. Frye, J. A. Blackmore, E. M. Bridge, R. Sawant, J. M. Hutson, and S. L. Cornish, Nat. Commun. **10**, 3104 (2019).
[34] M.-G. Hu, Y. Liu, D. D. Grimes, Y.-W. Lin, A. H. Gheorghe, R. Vexiau, N. Bouloufa-Maafa, O. Dulieu, T. Rosenband, and K.-K. Ni, Science **366**, 1111 (2019).
[35] B. Drews, M. Dei, K. Jachymski, Z. Idziaszek, and J. Hecker Denschlag, Nat. Commun. **8**, 14854 (2017).
[36] M. Mayle, B. P. Ruzic, and J. L. Bohn, Phys. Rev. A **85**, 062712 (2012).
[37] M. Mayle, G. Quéméner, B. P. Ruzic, and J. L. Bohn, Phys. Rev. A **87**, 012709 (2013).
[38] E. B. Norrgard, D. J. McCarron, M. H. Steinecker, M. R. Tarbutt, and D. DeMille, Phys. Rev. Lett. **116**, 063004 (2016).
[39] D. J. McCarron, M. H. Steinecker, Y. Zhu, and D. DeMille, Phys. Rev. Lett. **121**, 013202 (2018).
[40] L. Anderegg, B. L. Augenbraun, Y. Bao, S. Burchesky, L. W. Cheuk, W. Ketterle, and J. M. Doyle, Nat. Phys. **14**, 890 (2018).
[41] L. W. Cheuk, L. Anderegg, B. L. Augenbraun, Y. Bao, S. Burchesky, W. Ketterle, and J. M. Doyle, Phys. Rev. Lett. **121**, 083201 (2018).

[42] L. Anderegg, L. W. Cheuk, Y. Bao, S. Burchesky, W. Ketterle, K.-K. Ni, and J. M. Doyle, Science **365**, 1156 (2019).
[43] P. Xu, J. Yang, M. Liu, X. He, Y. Zeng, K. Wang, J. Wang, D. J. Papoular, G. V. Shlyapnikov, and M. Zhan, Nat. Commun. **6**, 7803 (2015).
[44] L. R. Liu, J. D. Hood, Y. Yu, J. T. Zhang, N. R. Hutzler, T. Rosenband, and K.-K. Ni, Science **360**, 900 (2018).
[45] P. Sompet, S. S. Szigeti, E. Schwartz, A. S. Bradley, and M. F. Andersen, Nat. Commun. **10**, 1889 (2019).
[46] J. D. Hood, Y. Yu, Y.-W. Lin, J. T. Zhang, K. Wang, L. R. Liu, B. Gao, and K.-K. Ni, Phys. Rev. Research **2**, 023108 (2020).
[47] See the Supplemental Material at http://link.aps.org/supplemental/10.1103/PhysRevLett.125.043401 for experimental details, which includes Refs. [33,41,48–50].
[48] Z. Idziaszek and P. S. Julienne, Phys. Rev. Lett. **104**, 113202 (2010).
[49] M. D. Frye, P. S. Julienne, and J. M. Hutson, New J. Phys. **17**, 045019 (2015).
[50] C. Tuchendler, A. M. Lance, A. Browaeys, Y. R. P. Sortais, and P. Grangier, Phys. Rev. A **78**, 033425 (2008).
[51] E. R. Meyer and J. L. Bohn, Phys. Rev. A **83**, 032714 (2011).
[52] T. Karman (private communication).
[53] Y. Liu, M.-G. Hu, M. A. Nichols, D. D. Grimes, T. Karman, H. Guo, and K.-K. Ni, Nat. Phys., https://doi.org/10.1038/s41567-020-0968-8 (2020).
[54] T. V. Tscherbul, J. Kłos, and A. A. Buchachenko, Phys. Rev. A **84**, 040701(R) (2011).
[55] M. Morita, J. Kłos, A. A. Buchachenko, and T. V. Tscherbul, Phys. Rev. A **95**, 063421 (2017).
[56] A. Christianen, M. W. Zwierlein, G. C. Groenenboom, and T. Karman, Phys. Rev. Lett. **123**, 123402 (2019).
[57] P. D. Gregory, J. A. Blackmore, S. L. Bromley, and S. L. Cornish, Phys. Rev. Lett. **124**, 163402 (2020).
[58] W. S. Bakr, P. M. Preiss, M. E. Tai, R. Ma, J. Simon, and M. Greiner, Nature (London) **480**, 500 (2011).
[59] I. Kozyryev, L. Baum, K. Matsuda, and J. M. Doyle, Chem. Phys. Chem. **17**, 3641 (2016).
[60] J. A. Blackmore, L. Caldwell, P. D. Gregory, E. M. Bridge, R. Sawant, J. Aldegunde, J. Mur-Petit, D. Jaksch, J. M. Hutson, B. E. Sauer, M. R. Tarbutt, and S. L. Cornish, Quantum Sci. Technol. **4**, 014010 (2018).

Correction: The value for the loss rate for ground-state molecules provided in the abstract as well as in text preceding Fig. 3 has been fixed. The previously published Fig. 4 contained a corresponding error and has been replaced.